Topologically protected Casimir effect for lattice fermions

C. W. J. Beenakker

Instituut-Lorentz, Universiteit Leiden, P.O. Box 9506, 2300 RA Leiden, The Netherlands

The electromagnetic Casimir effect has a fermionic counterpart in topological insulators: Zero-point fluctuations of a massless Dirac fermion field mediate a force between magnetic scatterers. The Casimir force is insensitive to disorder that preserves the topological protection of an unpaired Dirac cone. The protection may be broken if the Dirac equation is discretized, and an exponential suppression of the Casimir effect will result if a gap opens at the Dirac point. Here, we show how this lattice artifact may be avoided, by applying a recently developed local discretization of the Euclidean action that does not suffer from the fermion-doubling obstruction of local discretizations of the Hamiltonian.

I. INTRODUCTION

The Casimir effect [1–3] is the attractive force between two metal plates in vacuum due to zero-point fluctuations of the electromagnetic field. The radiation pressure is lower in between the plates than outside and pulls the plates together. This generic quantum effect has an electronic analog for massless Dirac fermions. Early studies of the fermionic Casimir effect were in the context of high-energy physics [4–7]. The emergence of massless electrons in graphene and topological insulators has created applications in condensed matter physics [8–10].

The Casimir force of a massless field decays as a power law with distance, however, it is suppressed exponentially if the low-energy excitations acquire a nonzero mass, meaning that a gap at the Dirac point opens up in the spectrum [11–13]. Dirac fermions remain massless provided that both these conditions are satisfied [14,15]: (1) The low-energy spectrum has only a single Dirac cone (i.e., there is only a single species of low-energy excitations); and (2) chiral symmetry and time-reversal symmetry are not both broken.

In graphene there are two Dirac cones at opposite corners of the Brillouin zone (valley degeneracy). Hence short-range disorder that couples these two cones via a large momentum transfer can open up a gap at the Dirac point and suppress the Casimir force. In contrast, on the surface of a topological insulator there is a single unpaired Dirac cone. The Casimir effect in a topological insulator can therefore not be suppressed by (time-reversal symmetry preserving) electrostatic disorder.

This topological protection of the Casimir effect may be compromised if the Dirac equation is discretized [16–19]. A local and symmetry-preserving discretization of the Dirac Hamiltonian necessarily introduces a second Dirac cone [20], an obstruction known as fermion doubling [21]. One way to work around this obstruction is to embed the Dirac Hamiltonian in a higher-dimensional lattice [22,23]. This is how a three-dimensional (3D) topological insulator allows for an unpaired Dirac cone on its 2D surface, or how a 2D quantum spin Hall insulator has an unpaired Dirac cone on its 1D edge.

Here, we present an alternative, dimension-preserving, route to a topologically protected Casimir force for lattice fermions. Following Ref. [24], space-time is discretized to obtain an Euclidean action that is local, preserves fundamental symmetries, and has only a single species of low-energy excitations. The second Dirac cone, required by a no-go theorem [20], is pushed to high energies by the time discretization, and as we will demonstrate does not affect the Casimir force. In particular, we show that short-range disorder has no effect on the power-law distance dependence (no exponential suppression because the low-energy excitations remain massless).

The outline of the paper is as follows: In the next section we give the scattering formulation of the fermionic Casimir effect on a space-time lattice, in terms of the tangent discretization of derivative operators [25,26]. The metallic plates of the electromagnetic effect are replaced by "mass barriers" [4], which in a topological insulator correspond to magnetic scatterers. The scattering matrix on the lattice is calculated in Sec. III, and then in Secs. IV–VI the Casimir force is obtained for various cases: extended mass barriers and "mass spikes" [7], in 1D and 2D. The topological protection is demonstrated in Sec. VII. We conclude in Sec. VIII.

II. CASIMIR EFFECT ON A SPACE-TIME LATTICE

We adapt the scattering formulation of the Casimir effect in the continuum [27–33] to discrete space and discrete (imaginary) time. We first consider one single spatial dimension (1D case), relevant for the quantum spin Hall edge, turning later to the 2D case relevant for the surface of a topological insulator.

A. Dirac fermions confined by mass barriers

We consider the Dirac Hamiltonian

$$\mathcal{H} = -iv_{\mathrm{F}}\sigma_x\partial_x + \mu(x)\sigma_z, \tag{2.1}$$

with v_F the Fermi velocity and Pauli spin matrices σ_α. The Fermi level is fixed at the Dirac point, $E = 0$. We set $\hbar$ to unity and denote partial derivatives by $\partial_x \equiv \partial/\partial x$.

Low-energy excitations are confined to a segment of length L by a pair of mass barriers of length L_μ,

$$\mu(x) = \begin{cases} \mu_L & \text{if } -L_\mu < x < 0, \\ \mu_R & \text{if } L < x < L + L_\mu, \\ 0 & \text{otherwise.} \end{cases} \quad (2.2)$$

On the surface of a topological insulator such a mass profile can be produced by the perpendicular magnetization of a magnetic insulator. The magnetization breaks time-reversal symmetry and opens a gap in the spectrum, causing the low-energy excitations to decay for $x < 0$ and for $x > L$. In the intermediate region $0 < x < L$ the spectrum remains gapless.

The confinement is only effective at energies $E \lesssim \mu_L, \mu_R$. At higher energies the mass barriers are transparent. This is a physical requirement. As we will see shortly, it is also a technical requirement [34] for our method to work around the fermion-doubling obstruction.

The transmission amplitude from one barrier to the other is $t(E)$, the same for transmission from left to right and from right to left. The reflection amplitudes from the left and right barriers are $r_L(E)$ and $r_R(E)$, respectively. The product of these scattering amplitudes gives the L-dependent contribution to the density of states, according to [29]

$$\rho(E) = -\frac{1}{\pi} \text{Im} \frac{d}{dE} \ln[1 - \Xi(E + i0^+)],$$
$$\Xi(E) = r_L(E) r_R(E) t(E)^2. \quad (2.3)$$

Our objective is to compute the L dependence of the free energy $\mathcal{F}$, in equilibrium at inverse temperature $\beta = 1/k_B T$, to obtain the Casimir force $F_C = -d\mathcal{F}/dL$.

B. Tangent fermion discretization

The free energy has the path integral expression [35,36]

$$\mathcal{F} = -\beta^{-1} \ln Z,$$
$$Z = \int \mathcal{D}\chi \int \mathcal{D}\bar{\chi} \exp\left(-\int_0^\beta dt \int dx \, \mathcal{L}[\chi, \bar{\chi}]\right), \quad (2.4)$$

in terms of the anticommuting (Grassmann) spinor fields χ, $\bar{\chi}$ and the Euclidean Lagrangian

$$\mathcal{L}[\chi, \bar{\chi}] = \bar{\chi}(x, t)(\partial_t + \mathcal{H})\chi(x, t). \quad (2.5)$$

The Lagrangian is integrated along the interval $0 < it < i\beta$ on the imaginary-time axis, with antiperiodic boundary conditions: $\chi(x, \beta) = -\chi(x, 0)$.

In the tangent fermion approach of Ref. [24], space and imaginary time are discretized in units of a and τ, respectively, chosen such that β/τ, L/a, and L_μ/a are integers. The space-time lattice consists of the points $it_n = in\tau$, $n = 0, 1, 2 \ldots \beta/\tau - 1$, on the imaginary-time axis and $x_n = na$, $n \in \mathbb{Z}$ on the real-space axis.

The discretized Lagrangian is given by

$$\mathcal{L}[\chi, \bar{\chi}] = \bar{\chi}[-(2/\tau)i \tan(\hat{\omega}\tau/2) + \mathcal{H}]\chi, \quad (2.6)$$

$$\mathcal{H} = (2v_F/a)\sigma_x \tan(\hat{k}a/2) + \mu(x)\sigma_z, \quad (2.7)$$

with $\hat{k} = -i\partial_x$, $\hat{\omega} = i\partial_t$. The fields χ, $\bar{\chi}$ are nonlocally coupled by the tangent operators, but a linear transformation produces a local Lagrangian [24].

The dispersion relation

$$\tan^2(\omega\tau/2) = \gamma^2 \tan^2(ka/2), \quad \gamma = v_F\tau/a, \quad (2.8)$$

has two Dirac points in the Brillouin zone: one Dirac point at low energies, $\omega\tau = ka = 0$, and a second Dirac point at high energies, $\omega\tau = ka = \pi$. The mass barriers do not confine the Dirac field at high energies, so we can expect that the second Dirac point will not affect the Casimir force. This is how the fermion-doubling obstruction [20] is avoided, without compromising the locality or symmetry of the Lagrangian.

Evaluation of the Gaussian path integral (2.4) gives the free energy

$$\mathcal{F} = -\beta^{-1} \sum_{n=0}^{\beta/\tau-1} \int_{-\infty}^{\infty} dE \, \rho(E) \ln[E - (2/\tau)i\tan(\omega_n\tau/2)], \quad (2.9)$$

in terms of a *finite* sum over the Matsubara frequencies $\omega_n = (2n + 1)\pi/\beta$. The pole in the tangent dispersion is avoided by choosing the integer β/τ even.

We substitute Eq. (2.3) and perform a partial integration,

$$\mathcal{F} = -\frac{1}{\pi\beta} \text{Im} \sum_{n=0}^{\beta/\tau-1} \int_{-\infty}^{\infty} dE \frac{\ln[1 - \Xi(E + i0^+)]}{E - (2/\tau)i\tan(\omega_n\tau/2)}. \quad (2.10)$$

We close the integration interval by a large contour in the upper half of the complex plane, to pick up the poles on the positive imaginary axis. The scattering amplitudes are analytic for $\text{Im} E > 0$ (no poles). We thus arrive at

$$\mathcal{F} = -\frac{2}{\beta} \text{Re} \sum_{n=1}^{\beta/2\tau-1} \ln[1 - \Xi(i\xi_n)],$$
$$\xi_n = (2/\tau)\tan(\omega_n\tau/2). \quad (2.11)$$

In what follows we will limit ourselves to zero temperature, when the sum over the Matsubara frequencies can be replaced by an integral,

$$\lim_{T\to 0} \mathcal{F} = -\frac{1}{\pi\tau} \text{Re} \int_0^\pi d\omega \ln[1 - \Xi(2i\tan(\omega/2))]. \quad (2.12)$$

The continuum formula [27–33] for the Casimir free energy is obtained if we replace $2\tan(\omega/2)$ by ω and integrate from 0 to ∞.

III. TANGENT FERMION SCATTERING AMPLITUDES

The eigenvalue equation $\mathcal{H}\Psi = E\Psi$ in the tangent discretization (2.7) is nonlocal, coupling the wave function $\Psi_n \equiv \Psi(x = na)$ at arbitrarily distant lattice points. This nonlocality is only apparent [25,37], and it can be removed by the substitution

$$\Psi_n = \tfrac{1}{2}(\Phi_n + \Phi_{n+1}). \quad (3.1)$$

The x dependence of the Φ field is governed by a *local* relation [26,38] $\Phi_{n+1} = M_n(E)\phi_n$ with transfer matrix

$$M_n = (1 - i\sigma_x U_n)^{-1}(1 + i\sigma_x U_n),$$
$$U_n = (a/2v_F)[E - \sigma_z \mu(x = na)]. \quad (3.2)$$

The transfer matrix from $x = 0$ to $x = L$ is given by $M_n^{L/a}$ with $\mu \equiv 0$. A right-moving state is an eigenstate of σ_x with eigenvalue $+1$, which gives the transmission amplitude

$$t(E) = \left(\frac{1 + \frac{1}{2}iEa/v_F}{1 - \frac{1}{2}iEa/v_F} \right)^{L/a}. \quad (3.3)$$

The calculation of the reflection amplitude from a mass barrier is a bit more complicated (see Appendix B). For a barrier of length L_μ and mass μ we find

$$\frac{1}{r(E)} = \frac{E}{\mu} + i \frac{v_F \Delta}{a\mu} \frac{\left(\frac{2+\Delta}{2-\Delta}\right)^{2L_\mu/a} + 1}{\left(\frac{2+\Delta}{2-\Delta}\right)^{2L_\mu/a} - 1},$$
$$\Delta(E) = \frac{a}{v_F}\sqrt{\mu^2 - E^2}. \quad (3.4)$$

The penetration depth ξ_μ into the barrier at $E = 0$ is given by

$$\frac{a}{\xi_\mu} = \ln\left| \frac{2 + \Delta_0}{2 - \Delta_0} \right| = \begin{cases} \Delta_0/4 & \text{if } \Delta_0 \ll 1, \\ 4/\Delta_0 & \text{if } \Delta_0 \gg 1, \end{cases} \quad (3.5)$$

with $\Delta_0 = a|\mu|/v_F$. The large-Δ_0 behavior is a lattice artifact, and only the regime $|\mu| \lesssim v_F/a$ is physical.

IV. CASIMIR FORCE BETWEEN EXTENDED MASS BARRIERS

In the limit $L_\mu \to \infty$ of an infinitely extended mass barrier the reflection amplitude (3.4) simplifies to

$$\lim_{L_\mu \to \infty} r(i\omega) = i\omega/\mu - i\mu^{-1}\sqrt{\mu^2 + \omega^2}. \quad (4.1)$$

We substitute Eqs. (3.3) and (4.1) for the transmission and reflection amplitudes into the free-energy formula (2.12),

$$\mathcal{F} = -\frac{1}{\pi\tau} \int_0^\pi d\omega \ln \left[1 + \left(\xi/\mu_L\tau - \mu_L^{-1}\sqrt{\mu_L^2 + (\xi/\tau)^2} \right) \right.$$
$$\left. \times \left(\xi/\mu_R\tau - \mu_R^{-1}\sqrt{\mu_R^2 + (\xi/\tau)^2} \right) \left(\frac{1 - \frac{1}{2}\xi/\gamma}{1 + \frac{1}{2}\xi/\gamma} \right)^{2L/a} \right], \quad (4.2)$$

with $\xi = 2\tan(\omega/2)$, $\gamma = v_F\tau/a$. In Fig. 1 we compare this with the continuum result,

$$\mathcal{F}_{\text{cont}} = -\frac{1}{\pi} \int_0^\infty d\omega \ln \left[1 + \left(\omega/\mu_L - \mu_L^{-1}\sqrt{\mu_L^2 + \omega^2} \right) \right.$$
$$\left. \times \left(\omega/\mu_R - \mu_R^{-1}\sqrt{\mu_R^2 + \omega^2} \right) e^{-2\omega L/v_F} \right]. \quad (4.3)$$

The two match closely.

In the large-L limit Eq. (4.2) tends to

$$\mathcal{F}_\infty = -\frac{\hbar v_F}{\pi L} \int_0^\infty dx \ln[1 - r_L(0)r_R(0)e^{-2x}]. \quad (4.4)$$
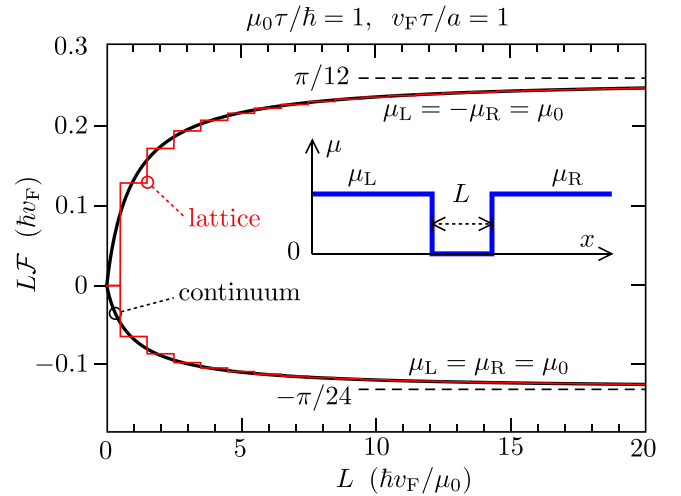

FIG. 1. Dependence of the zero-temperature free energy $\mathcal{F}$ of 1D massless fermions on the separation L of a pair of mass boundaries. The derivative $-d\mathcal{F}/dL$ is the Casimir force on the barriers. The force is attractive if the two magnetizations μ_L, μ_R have the same sign (lower curves), and repulsive if they have the opposite sign (upper curves). The plot compares the result (4.2) on a lattice (red) with the continuum result (4.3) (black). [The dashed lines are the large-L asymptotes (4.5).] The space-time lattice constants a and τ have been chosen such that $\mu_0\tau/\hbar = 1 = v_F\tau/a$. The inset shows the magnetization profile $\mu(x)$ that produces the mass boundaries.

We thus recover the familiar values [4,8]

$$\mathcal{F}_\infty = \frac{\hbar v_F}{L} \times \begin{cases} -\pi/24 & \text{if } \text{sgn}(\mu_L\mu_R) = +1, \\ +\pi/12 & \text{if } \text{sgn}(\mu_L\mu_R) = -1, \end{cases} \quad (4.5)$$

The corresponding Casimir force $F_C = -d\mathcal{F}/dL$ decays as $1/L^2$, attractive or repulsive depending on whether μ_L and μ_R have the same or opposite sign.
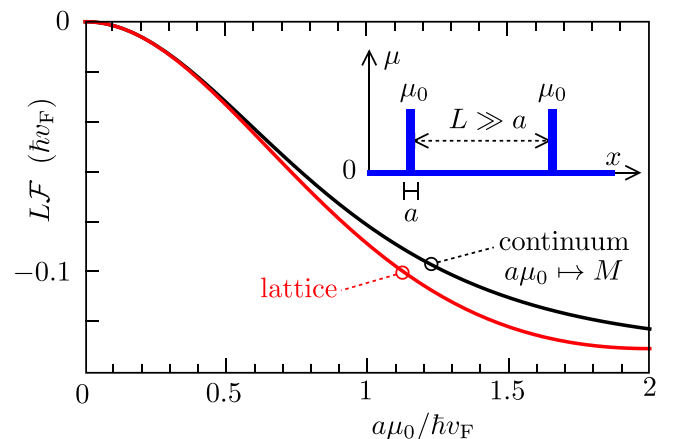

FIG. 2. Mass dependence of the Casimir free energy for a delta function mass profile $\mu(x) = M\delta(0) + M\delta(x - L)$ in the continuum [black curve, Eq. (5.3)], modeled by two barriers of height $\mu_0 \equiv M/a$ and width a on the lattice [red curve, Eq. (5.2)]. The agreement is precise for lattice constants a much smaller than both L and $\hbar v_F/\mu_0$.
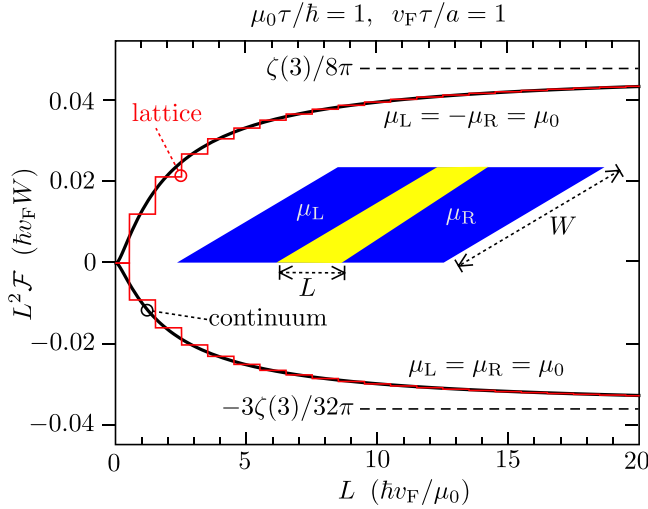
FIG. 3. Same as Fig. 1, but for the 2D case, computed from Eqs. (6.1) and (6.2). The dashed lines are the large-L asymptotes (6.3).

V. CASIMIR FORCE BETWEEN MASS SPIKES

A delta function mass profile, a "mass spike" [7], is represented on the lattice by a mass barrier which is one lattice constant long. This is a model for a magnetic impurity on the quantum spin Hall edge. The reflection amplitude follows from Eq. (3.4) with $L_\mu = a$, which simplifies to

$$r_X(E) = \frac{4ia\mu_X/v_F}{(aE/v_F + 2i)^2 - (a\mu_X/v_F)^2}, \quad X \in \{L, R\}. \quad (5.1)$$

Substitution into Eq. (4.4) gives for $L \gg a$ the Casimir free energy

$$\mathcal{F}_\infty = \frac{\hbar v_F}{2\pi L}\text{Li}_2(-M_L M_R), \quad M_X = \frac{4a\mu_X/v_F}{4 + (a\mu_X/v_F)^2}, \quad (5.2)$$

with Li_2 a polylogarithm. This can be compared with the continuum result [7,39] for the mass profile $\mu(x) = M\delta(x) + M\delta(x - L)$,

$$\mathcal{F}_{\text{cont}} = \frac{\hbar v_F}{2\pi L}\text{Li}_2[-\tanh^2(M/v_F)]. \quad (5.3)$$

As shown in Fig. 2, the two expressions agree in the small-mass regime $M \equiv a\mu_0 \ll v_F$.

To clarify the correspondence of the lattice and continuum formulas it is helpful to rewrite the lattice formula (5.2) for identical mass spikes as

$$\mathcal{F}_\infty = \frac{\hbar v_F}{2\pi L}\text{Li}_2[-\tanh^2(a\mu_{\text{eff}}/v_F)], \quad \mu_{\text{eff}} \equiv v_F/\xi_\mu, \quad (5.4)$$

with ξ_μ the lattice penetration depth from Eq. (3.5). Equation (5.4) corresponds to the continuum formula (5.3) if we identify M/a with the effective mass μ_{eff}.

VI. CASIMIR FORCE BETWEEN MASS BARRIERS ON A 2D SURFACE

These 1D expressions can readily be generalized to the 2D case. We consider a pair of mass barriers along the y axis, with the mass profile $\mu(x)$ given by Eq. (2.2). The transmission and reflection coefficients now depend both on energy E and on the transverse wave number k_y (which is a conserved quantity). We work out the case $L_\mu \to \infty$ of extended barriers.

Using the results for the reflection and transmission coefficients from Appendix B we obtain the free energy

$$\mathcal{F} = -\frac{W}{\pi\tau}\int_0^\pi d\omega \int_{-\pi/a}^{\pi/a} \frac{dk_y}{2\pi} \ln\left[1 + \frac{1}{\mu_L\mu_R\tau^2}(\sqrt{(\gamma\xi_y)^2 + \xi^2} - \sqrt{(\mu_L\tau)^2 + (\gamma\xi_y)^2 + \xi^2})\right.$$

$$\left. \times (\sqrt{(\gamma\xi_y)^2 + \xi^2} - \sqrt{(\mu_R\tau)^2 + (\gamma\xi_y)^2 + \xi^2})\left(\frac{2\gamma - \sqrt{(\gamma\xi_y)^2 + \xi^2}}{2\gamma + \sqrt{(\gamma\xi_y)^2 + \xi^2}}\right)^{2L/a}\right], \quad (6.1)$$

with $\xi = 2\tan(\omega/2)$ and $\xi_y = 2\tan(ak_y/2)$. This expression includes the contributions from both propagating and decaying modes in the interbarrier region.

In Fig. 3 we compare Eq. (6.1) with the continuum result,

$$\mathcal{F}_{\text{cont}} = -\frac{W}{\pi}\int_0^\infty d\omega \int_{-\infty}^\infty \frac{dk_y}{2\pi} \ln\left[1 + \frac{1}{\mu_L\mu_R}(\sqrt{(v_F k_y)^2 + \omega^2} - \sqrt{\mu_L^2 + (v_F k_y)^2 + \omega^2})\right.$$

$$\left. \times \left(\sqrt{(v_F k_y)^2 + \omega^2} - \sqrt{\mu_R^2 + (v_F k_y)^2 + \omega^2}\right)\exp\left(-\frac{2L}{v_F}\sqrt{(v_F k_y)^2 + \omega^2}\right)\right]. \quad (6.2)$$

The two match closely, both tending to the large-L limit of Appendix C,

$$\mathcal{F}_\infty = -\frac{\hbar v_F W}{2\pi L^2}\int_0^\infty r\,dr\,\ln[1 + \text{sgn}(\mu_L\mu_R)e^{-2r}]$$

$$= \frac{\hbar v_F W}{L^2} \times \begin{cases} -3\zeta(3)/32\pi & \text{if } \text{sgn}(\mu_L\mu_R) = +1, \\ +\zeta(3)/8\pi & \text{if } \text{sgn}(\mu_L\mu_R) = -1. \end{cases} \quad (6.3)$$

VII. TOPOLOGICAL PROTECTION OF THE CASIMIR FORCE

To test the topological protection of the fermionic Casimir effect we apply an electrostatic potential $V(x)$ to the interbarrier region, in the 1D case with extended mass boundaries. This potential preserves time-reversal symmetry, so the fermions should remain massless.

We consider the staggered potential $V(x) = V_0 \cos(\pi x/a)$, so $V = \pm V_0$ on even- and odd-numbered sites, which keeps the Fermi level at zero energy. (A nonzero Fermi wave vector k_F would introduce $\sin k_F L$ oscillations in the Casimir force [40,41].)

The staggered potential modifies the tangent fermion transmission amplitude by a $\pm V_0$ displacement of the energy,

$$t(E) = \left(\frac{1 + \frac{1}{2} i (E - V_0) a / v_F}{1 - \frac{1}{2} i (E - V_0) a / v_F} \right)^{L/2a}$$
$$\times \left(\frac{1 + \frac{1}{2} i (E + V_0) a / v_F}{1 - \frac{1}{2} i (E + V_0) a / v_F} \right)^{L/2a}, \quad (7.1)$$

for L/a an even integer. On the imaginary energy axis we have

$$t[2i \tan(\omega/2)]$$
$$= \left(1 - \frac{8 \sin \omega}{(V_0 a / v_F)^2 \cos^2(\omega/2) + 4 \sin \omega + 4} \right)^{L/2a}$$
$$\to \exp \left(-\frac{\omega L/a}{1 + (V_0 a / 2 v_F)^2} \right), \quad (7.2)$$

in the large-L, small-ω limit.

The zero-temperature free energy, in the limit $L, L_\mu \to \infty$, is given by

$$\mathcal{F}_\infty = -\frac{1}{\pi \tau} \int_0^\infty d\omega \ln[1 + \text{sgn}(\mu_L \mu_R) e^{-2\omega L_{\text{eff}}/a}],$$
$$L_{\text{eff}} = \frac{L}{1 + (V_0 a / 2 v_F)^2}, \quad (7.3)$$

which evaluates to the result (4.5) with a renormalized length $L \mapsto L_{\text{eff}}$.

As anticipated, the power-law L dependence of the Casimir force is not affected by the staggered potential in the tangent fermion discretization. In contrast, if a discretization scheme allows a gap E_{gap} to open at the Dirac point, then the Casimir force decays $\propto e^{-E_{\text{gap}} L / v_F}$ with increasing L [11–13]. The gap due to the staggered potential is different for different types of lattice fermions [26,42], of order V_0 for naive fermions and of order $V_0^2 a / v_F$ for other discretization schemes (Wilson fermions, SLAC fermions, Kogut-Susskind fermions [21], see Appendix D).

VIII. CONCLUSION

In summary, we have shown that it is possible to study the fermionic Casimir effect on a lattice without giving up on the topological protection of an unpaired Dirac cone, and without the need to embed the lattice in higher-dimensional space. The ingredients that permit to work around the fermion-doubling obstruction are as follows: (1) the tangent fermion space-time discretization that pushes the spurious second Dirac cone to high energies [24]; and (2) the use of the physical condition that high-energy fermions are not confined by mass barriers and therefore do not contribute to the Casimir force.

On the quantum spin Hall edge the Casimir force between magnetic impurities decays slowly $\propto 1/L^2$, unaffected by electrostatic disorder. For a Fermi velocity of 10^6 m/s this corresponds to an interaction energy of 10 meV at a separation of 10 nm, which may have measurable consequences, such as the aggregation of magnetic impurities with parallel magnetization (as in the analogous case in graphene or carbon nanotubes [8,9]). Our lattice fermion approach should allow for efficient computer simulations of the Casimir effect with electron-electron interactions [43].

APPENDIX A: INFINITE-MASS BOUNDARY CONDITION IS INCOMPATIBLE WITH THE TANGENT FERMION DISCRETIZATION

In the infinite-mass limit, when the mass boundaries may be considered impenetrable at all energies, we may replace them by a boundary condition on the modes in the interbarrier region. That approach is taken in Refs. [17,18], for several types of lattice fermions. We have found that the infinite-mass boundary condition is not appropriate for tangent fermions. For that discretization scheme it is essential to retain the physical requirement that the barriers are transparent at high energies. We show this for the 1D case with $\text{sgn}(\mu_L \mu_R) = +1$.

The infinite-mass boundary condition for tangent fermions implies the energy quantization

$$E_m = (2/\tau) \tan[(m + 1/2)\pi a/L],$$
$$m = -L/a, \dots, -1, 0, 1, \dots L/a - 1. \quad (A1)$$

The zero-temperature free energy (2.9) is then given by

$$\mathcal{F} = -\frac{1}{2\pi \tau} \sum_{m=-L/a}^{L/a-1} \int_0^{2\pi} d\omega \ln \{2\gamma \tan[(m + 1/2)\pi a/2L] - 2i \tan(\omega/2)\}$$
$$= -\frac{2L}{a\tau} \ln 2 + \sum_{m=0}^{L/a-1} f(m + 1/2), \quad f(x) = -\frac{2}{\tau} \ln[1 + \gamma \tan(x\pi a/2L)]. \quad (A2)$$

The regularized zero-point energy is the difference between the sum and integral,

$$\delta\mathcal{F} = \sum_{m=0}^{L/a-1} f(m+1/2) - \int_0^{L/a} f(x)dx = \mathcal{F} - L \lim_{L\to\infty} L^{-1}\mathcal{F}. \tag{A3}$$

We use the Abel-Plana formula [44]

$$\sum_{n=\lceil A-\nu\rceil}^{\lfloor B-\nu\rfloor} f(n+\nu) - \int_A^B f(x)dx = \Delta(A,\nu) + \Delta(B,\nu) - Q(A,\nu) + Q(B,\nu), \tag{A4a}$$

$$\Delta(A,\nu) = \begin{cases} \frac{1}{2}f(A) & \text{if } A-\nu \in \mathbb{Z}, \\ 0 & \text{otherwise,} \end{cases} \tag{A4b}$$

$$Q(A,\nu) = \frac{1}{i}\int_0^\infty dy \left[\frac{f(A+iy)}{e^{2\pi y - 2\pi i(A-\nu)} - 1} - \frac{f(A-iy)}{e^{2\pi y + 2\pi i(A-\nu)} - 1} \right], \tag{A4c}$$

for $A, B, \nu \in \mathbb{R}$.

Applied to Eq. (A2) (with $A=0$, $B=L/a$, $\nu=1/2$) this gives the zero-point energy

$$\delta\mathcal{F} = -\frac{4}{\tau}\int_0^\infty dy \frac{\arctan[\gamma \tanh(y\pi a/2L)]}{e^{2\pi y} + 1} + \frac{4}{\tau}\int_0^\infty dy \frac{\arctan[\gamma \coth(y\pi a/2L)]}{e^{2\pi y} + 1}$$

$$= \frac{1}{\tau}\ln 2 - \frac{v_\mathrm{F}}{L}\frac{\pi(\gamma^2+1)}{24\gamma^2} + O(L^{-2}). \tag{A5}$$

The L-independent offset does not contribute to the Casimir force and can be ignored. The term that decays as $1/L$ only attains the correct prefactor (4.5) when $\gamma = v_\mathrm{F}\tau/a \to \infty$, so for vanishing lattice constant a. For finite γ the tangent fermion discretization overestimates the Casimir force in the infinite-mass limit, because of spurious contributions from high-energy modes at the edge of the Brillouin zone. This complication is avoided in the scattering approach from the main text, because there the mass barriers are transparent at high energies, hence the spurious modes are not confined and do not contribute to the Casimir force.

APPENDIX B: SCATTERING OF TANGENT FERMIONS BY A MASS BARRIER

We compute the tangent fermion reflection and transmission matrices for a mass barrier. We consider a 2D system, such as the surface of a topological insulator, with the barrier oriented along the y axis. The mass profile $\mu(x)$ depends only on x, so momentum k_y parallel to the boundary is conserved.

The transfer matrix M_n from $x = na$ to $x = (n+1)a$ is given by [26,38]

$$M_n = \left(1 - i\sigma_x U_n - \tfrac{1}{2}\sigma_z\xi_y\right)^{-1}\left(1 + i\sigma_x U_n + \tfrac{1}{2}\sigma_z\xi_y\right), \tag{B1a}$$

$$U_n = (a/2v_\mathrm{F})[E - \sigma_z\mu(x=na)], \quad \xi_y = 2\tan(ak_y/2). \tag{B1b}$$

[The 1D Eq. (3.2) corresponds to $k_y = 0$.] The full transfer matrix through the barrier, of length L_μ an integer multiple of the lattice constant a, is $M_n^{L_\mu/a}$.

The eigenstates of M_n for $\mu = 0$ are

$$\chi_+ = 2^{-1/2}(\sqrt{1 - (\gamma\xi_y/E\tau)^2} - i\gamma\xi_y/E\tau, 1),$$

$$\chi_- = 2^{-1/2}(1, -\sqrt{1 - (\gamma\xi_y/E\tau)^2} + i\gamma\xi_y/E\tau). \tag{B2}$$

For $|\gamma\xi_y/E\tau| < 1$ these are states which carry the same current in opposite directions,

$$\langle\chi_\pm|\sigma_x|\chi_\pm\rangle = \pm\sqrt{1 - (\gamma\xi_y/E\tau)^2}, \tag{B3}$$

so they can serve as the basis of incoming and outgoing states for the scattering matrix.

We transform the transfer matrix to the new basis,

$$\tilde{M}_n = \Omega^{-1}M_n\Omega, \quad \Omega = \begin{pmatrix} \chi_+ \\ \chi_- \end{pmatrix}^\top, \tag{B4}$$

and then find the scattering matrix S from

$$(\tilde{M}_n)^{L_\mu/a} = \begin{pmatrix} m_{11} & m_{12} \\ m_{21} & m_{22} \end{pmatrix} \Rightarrow$$

$$S = \begin{pmatrix} -m_{21}/m_{22} & 1/m_{22} \\ m_{11} - m_{12}m_{21}/m_{22} & m_{12}/m_{22} \end{pmatrix} \equiv \begin{pmatrix} r & t \\ t' & r' \end{pmatrix}. \tag{B5}$$

After some algebra we thus obtain the reflection and transmission coefficients

$$\frac{1}{r} = \frac{1}{r'} = \frac{\varepsilon}{\mu} + i\frac{v_\mathrm{F}\Delta}{a\mu}\frac{Q^2+1}{Q^2-1}, \tag{B6}$$

$$\frac{1}{t} = \frac{1}{t'} = \frac{1}{2}(Q + 1/Q) - \frac{1}{2}i\frac{a\varepsilon}{v_\mathrm{F}\Delta}(Q - 1/Q), \tag{B7}$$

with the definitions

$$\varepsilon = E\sqrt{1 - (\gamma \xi_y / E\tau)^2}, \tag{B8a}$$

$$\Delta = \frac{a}{v_F}\sqrt{\mu^2 + (\gamma \xi_y/\tau)^2 - E^2}, \tag{B8b}$$

$$Q = \left(\frac{2+\Delta}{2-\Delta}\right)^{L_\mu/a}. \tag{B8c}$$

For $k_y = 0$ Eq. (B6) reduces to Eq. (3.4).

We note the large-L_μ limit of the reflection coefficient for $E = i\omega$ on the imaginary axis,

$$\lim_{L_\mu \to \infty} r(i\omega) = \lim_{Q^2 \to \infty} r(i\omega)$$

$$= \frac{i\omega}{\mu}\sqrt{1 + (\gamma \xi_y/\omega\tau)^2}$$

$$- \frac{i}{\mu}\sqrt{\mu^2 + (\gamma \xi_y/\tau)^2 + \omega^2}, \tag{B9}$$

generalizing Eq. (4.1) to $k_y \neq 0$.

The transmission coefficient through a massless region of length L follows from Eq. (B7) with $\mu = 0$,

$$\lim_{\mu \to 0} t(E) = \left(\frac{1 + \frac{1}{2}i\varepsilon a/v_F}{1 - \frac{1}{2}i\varepsilon a/v_F}\right)^{L/a}, \tag{B10}$$

which for $k_y = 0$ reduces to Eq. (3.3).

APPENDIX C: FERMIONIC CASIMIR FORCE ON WIDELY SEPARATED MASS BOUNDARIES

To compare with the literature on the fermionic Casimir force we record the limiting expressions we obtain for the case $L_\mu, L \to \infty$ of extended and widely separated mass barriers.

In the scattering formulation the zero-point energy in $d + 1$-dimensional continuous space-time is given by an integral over the imaginary frequency $i\omega$ and a $d - 1$-dimensional integral over the transverse wave vector $\boldsymbol{k}_\parallel$,

$$\mathcal{F}_\infty = -\hbar \int_0^\infty \frac{d\omega}{\pi} \int \frac{d\boldsymbol{k}_\parallel}{(2\pi)^{d-1}}$$

$$\times \ln[1 - r_L(i\omega, \boldsymbol{k}_\parallel) r_R(i\omega, \boldsymbol{k}_\parallel) e^{-2L\sqrt{(\omega/v_F)^2 + |\boldsymbol{k}_\parallel|^2}}]. \tag{C1}$$

This is the zero-temperature free energy per unit area of the mass barriers and for a single spin degree of freedom.

In the large-L limit we may replace the reflection coefficients r_L, r_R by their value $\pm i$ at $\omega = 0 = \boldsymbol{k}_\parallel$, where the sign $\pm i$ depends on the sign of the mass. Upon transformation to spherical coordinates we have the integral

$$\mathcal{F}_\infty = -\frac{\hbar v_F}{L^d} \frac{2\pi^{d/2}}{(2\pi)^d \Gamma(d/2)} \int_0^\infty r^{d-1} dr$$

$$\times \ln[1 + \mathrm{sgn}(\mu_L \mu_R) e^{-2r}], \tag{C2}$$

which evaluates to

$$\mathcal{F}_\infty = \frac{\hbar v_F}{L^d} \frac{\zeta(d+1)\Gamma(d)}{2^{3d-1}\pi^{d/2}\Gamma(d/2)}$$

$$\times \begin{cases} (1 - 2^d) & \text{if } \mathrm{sgn}(\mu_L \mu_R) = +1 \\ 2^d & \text{if } \mathrm{sgn}(\mu_L \mu_R) = -1. \end{cases} \tag{C3}$$

Specifically, the coefficient $c_d^\pm$ in $\mathcal{F}_\infty = c_d^\pm \hbar v_F / L^d$ for $d = 1, 2, 3$ and $\mathrm{sgn}(\mu_L \mu_R) = \pm 1$ equals

$$\{c_1^+, c_2^+, c_3^+\} = \left\{-\frac{\pi}{24}, -\frac{3\zeta(3)}{32\pi}, -\frac{7\pi^2}{5760}\right\},$$

$$\{c_1^-, c_2^-, c_3^-\} = \left\{+\frac{\pi}{12}, +\frac{\zeta(3)}{8\pi}, +\frac{\pi^2}{720}\right\}. \tag{C4}$$

The Casimir force $F_C = -d\mathcal{F}/dL$ on the barriers is attractive if $\mathrm{sgn}(\mu_L \mu_R) = +1$ and repulsive if $\mathrm{sgn}(\mu_L \mu_R) = -1$.

The formula (C3) for the attractive fermionic Casimir force was derived in Ref. [6] by a different method (zeta function regularization). The result for the repulsive case equals -2 times the bosonic result from Ref. [5].

APPENDIX D: COMPARISON WITH OTHER LATTICE FERMIONS

As derived in Ref. [42], a staggered potential $V(x) = V_0 \cos(\pi x/a)$ may cause a gap E_{gap} to open up at the zero-energy Dirac point. This causes an exponential suppression $\propto e^{-E_{\text{gap}}L/v_F}$ of the Casimir force [11–13]. For tangent fermions the Dirac fermions remain massless. We summarize the gap results for various other types [21] of 1D lattice fermions.

The staggered potential couples states at k_x and $k_x + \pi/a$, as described by the Hamiltonian

$$H_V(k_x) = \begin{pmatrix} H(k_x) & V_0/2 \\ V_0/2 & H(k_x + \pi/a) \end{pmatrix}. \tag{D1}$$

For a given lattice Hamiltonian H one thus obtains the following gap E_{gap} at $k_x = 0$ in the spectrum of H_V:

(1) naive fermions: $H(k_x) = (v_F/a)\sigma_x \sin ak_x \Rightarrow E_{\text{gap}} = V_0$;

(2) Wilson fermions: $H(k_x) = (v_F/a)\sigma_x \sin ak_x + m_0 \sigma_z (1 - \cos ak_x) \Rightarrow E_{\text{gap}} = \sqrt{4m_0^2 + V_0^2} - 2m_0$;

(3) Kogut-Susskind fermions: $H(k_x) = (v_F/a)[\sigma_x \sin ak_x + \sigma_y(1 - \cos ak_x)] \Rightarrow E_{\text{gap}} = \sqrt{4v_F^2/a^2 + V_0^2} - 2v_F/a$;

(4) SLAC fermions: $H(k_x) = -i(v_F/a)\sigma_x \ln e^{iak_x} \Rightarrow E_{\text{gap}} = \sqrt{\pi^2 v_F^2/a^2 + V_0^2} - \pi v_F/a$.

The resulting Casimir force decays as $e^{-L/\xi}$ with $\xi \propto 1/V_0$ for naive fermions and $\xi \propto 1/V_0^2$ in the other three cases.

All of this should be contrasted with

(5) tangent fermions: $H(k_x) = 2(v_F/a)\sigma_x \tan(ak_x/2) \Rightarrow E_{\text{gap}} = 0$,

where the Casimir force retains the power-law decay $\propto 1/L^2$.

[1] H. B. G. Casimir, On the attraction between two perfectly conducting plates, Proc. R. Neth. Acad. Arts Sci. **51**, 793 (1948).

[2] G. Plunien, B. Müller, and W. Greiner, The Casimir effect, Phys. Rep. **134**, 87 (1986).

[3] V. M. Mostepanenko and N. N. Trunov, *The Casimir Effect and its Applications* (Clarendon Press, Oxford, UK, 1997).

[4] K. Johnson, The M.I.T. bag model, Acta Phys. Pol. B **6**, 865 (1975).

[5] J. Ambjørn and S. Wolfram, Properties of the vacuum. I. Mechanical and thermodynamic, Ann. Phys. **147**, 1 (1983).

[6] R. D. M. De Paola, R. B. Rodrigues, and N. F. Svaiter, Casimir energy of massless Fermions in the slab-bag, Mod. Phys. Lett. A **14**, 2353 (1999).

[7] P. Sundberg and R. L. Jaffe, The Casimir effect for fermions in one dimension, Ann. Phys. **309**, 442 (2004).

[8] D. Zhabinskaya, J. M. Kinder, and E. J. Mele, Casimir effect for massless fermions in one dimension: A force-operator approach, Phys. Rev. A **78**, 060103(R) (2008).

[9] A. V. Shytov, D. A. Abanin, and L. S. Levitov, Long-range interaction between adatoms in graphene, Phys. Rev. Lett. **103**, 016806 (2009).

[10] B. S. Lu, The Casimir effect in topological matter, Universe **7**, 237 (2021).

[11] P. Hays, Vacuum fluctuations of a confined massive field in two dimensions, Ann. Phys. **121**, 32 (1979).

[12] E. Elizalde, F. C. Santos, and A. C. Tort, The Casimir energy of a massive fermionic field confined in a $d + 1$ dimensional slab-bag, Int. J. Mod. Phys. A **18**, 1761 (2003).

[13] K. Nakayama and K. Suzuki, Remnants of the nonrelativistic Casimir effect on the lattice, Phys. Rev. Res. **5**, L022054 (2023).

[14] M. Z. Hasan and C. L. Kane, Topological insulators, Rev. Mod. Phys. **82**, 3045 (2010).

[15] X.-L. Qi and S.-C. Zhang, Topological insulators and superconductors, Rev. Mod. Phys. **83**, 1057 (2011).

[16] A. Actor, I. Bender, and J. Reingruber, Casimir effect on a finite lattice, Fortschr. Phys. **48**, 303 (2000).

[17] T. Ishikawa, K. Nakayama, and K. Suzuki, Lattice-fermionic Casimir effect and topological insulators, Phys. Rev. Res. **3**, 023201 (2021).

[18] Y. V. Mandlecha and R. V. Gavai, Lattice fermionic Casimir effect in a slab bag and universality, Phys. Lett. B **835**, 137558 (2022).

[19] E. Flores, C. Ireland, N. Jamhour, V. Lasasso, N. Kurth, and M. Leinbach, Casimir force in discrete scalar fields I: 1D and 2D cases, arXiv:2309.00624.

[20] H. B. Nielsen and M. Ninomiya, A no-go theorem for regularizing chiral fermions, Phys. Lett. B **105**, 219 (1981).

[21] For an overview of methods to discretize the Dirac Hamiltonian, see D. Tong, Lecture notes: https://www.damtp.cam.ac.uk/user/tong/gaugetheory/4lattice.pdf, H. J. Rothe, *Lattice Gauge Theories: An Introduction* (World Scientific, Singapore, 2005), Chap. 4.

[22] T. Kimura, Domain-wall, overlap, and topological insulators, arXiv:1511.08286.

[23] A. Ziesen, I. C. Fulga, and F. Hassler, Geometry-independent tight-binding method for massless Dirac fermions in two dimensions, Phys. Rev. B **107**, 195409 (2023).

[24] V. A. Zakharov, J. Tworzydło, C. W. J. Beenakker, and M. J. Pacholski, Helical Luttinger liquid on a space-time lattice, arXiv:2401.10828.

[25] R. Stacey, Eliminating lattice fermion doubling, Phys. Rev. D **26**, 468 (1982).

[26] C. W. J. Beenakker, A. Donís Vela, G. Lemut, M. J. Pacholski, and J. Tworzydło, Tangent fermions: Dirac or Majorana fermions on a lattice without fermion doubling, Ann. Phys. **535**, 2300081 (2023).

[27] M. T. Jaekel and S. Reynaud, Casimir force between partially transmitting mirrors, J. Phys. I France **1**, 1395 (1991).

[28] O. Kenneth, Generalized Casimir energies for systems with arbitrary planar geometry, arXiv:hep-th/9912102.

[29] A. Lambrecht, P. A. Maia Neto, and S. Reynaud, The Casimir effect within scattering theory, New J. Phys. **8**, 243 (2006).

[30] O. Kenneth and I. Klich, Casimir forces in a T-operator approach, Phys. Rev. B **78**, 014103 (2008).

[31] S. J. Rahi, T. Emig, N. Graham, R. L. Jaffe, and M. Kardar, Scattering theory approach to electrodynamic Casimir forces, Phys. Rev. D **80**, 085021 (2009).

[32] S. Jamal Rahi, T. Emig, and R. L. Jaffe, Geometry and material effects in Casimir physics—Scattering theory, Lect. Notes Phys. **834**, 129 (2011).

[33] P. A. Maia Neto, F. S. S. Rosa, L. B. Pires, A. B. Moraes, A. Canaguier-Durand, R. Guérout, A. Lambrecht, and S. Reynaud, Scattering theory of the screened Casimir interaction in electrolytes, Eur. Phys. J. D **73**, 178 (2019).

[34] As an alternative to the scattering approach to the Casimir effect, one may assume infinitely high barriers and replace the reflection amplitude by a boundary condition on the confined fields. As we discuss in Appendix A, that alternative approach is not compatible with the tangent fermion discretization.

[35] G. D. Mahan, *Many-Particle Physics* (Springer, New York, 2000).

[36] A. Altland and B. Simons, *Condensed Matter Field Theory* (Cambridge University Press, Cambridge, UK, 2023).

[37] M. J. Pacholski, G. Lemut, J. Tworzydło, and C. W. J. Beenakker, Generalized eigenproblem without fermion doubling for Dirac fermions on a lattice, SciPost Phys. **11**, 105 (2021).

[38] J. Tworzydło, C. W. Groth, and C. W. J. Beenakker, Finite difference method for transport properties of massless Dirac fermions, Phys. Rev. B **78**, 235438 (2008).

[39] Equation (5.3) follows upon integration of Eq. (4.19) from Ref. [7], in the massless fermion limit $m \to 0$. A comparison with the earlier Eq. (4.17) indicates a typo in Eq. (4.19): The factor $(t^2 - m^2)$ in the denominator of the integrand should be replaced by $(t^2 - m^2) \sinh^2 \lambda$, so that the integrand becomes $-\frac{2td \sinh^2 \lambda}{\pi e^{2td} \cosh^2 \lambda + \pi \sinh^2 \lambda}$ in the $m \to 0$ limit.

[40] J. N. Fuchs, A. Recati, and W. Zwerger, Oscillating Casimir force between impurities in one-dimensional Fermi liquids, Phys. Rev. A **75**, 043615 (2007).

[41] K. Nakayama and K. Suzuki, Dirac/Weyl-node-induced oscillating Casimir effect, Phys. Lett. B **843**, 138017 (2023).

[42] A. Donís Vela, M. J. Pacholski, G. Lemut, J. Tworzydło, and C. W. J. Beenakker, Massless Dirac fermions on a space-time lattice with a topologically protected Dirac cone, Ann. Phys. **534**, 2200206 (2022).

[43] A. Recati, J. N. Fuchs, C. S. Peça, and W. Zwerger, Casimir forces between defects in one-dimensional quantum liquids, Phys. Rev. A **72**, 023616 (2005).

[44] For the Abel-Plana formula in the form of Eq. (A.4), see Appendix B of Ref. [17] and https://mathoverflow.net/q/459483/11260.